BioMetals 1998, **11**, 213–222

Metal ion binding to calmodulin: NMR and fluorescence studies

Hui Ouyang & Hans J. Vogel

Department of Biological Sciences, The University of Calgary, Calgary, Canada

Received 26 January 1998; accepted for publication 3 March 1998

Calmodulin is an important second messenger protein which is involved in a large variety of cellular pathways. Calmodulin is sensitive to fluctuations in the intracellular Ca^{2+} levels and is activated by the binding of four Ca^{2+} ions. In spite of the important role it plays in signal transduction pathways, it shows a surprisingly broad specificity for binding metal ions. Using ^{15}N-Gly biosynthetically-labelled calmodulin, we have studied the binding of different metal ions to calmodulin, including K^+, Na^+, Ca^{2+}, Mg^{2+}, Zn^{2+}, Cd^{2+}, Pb^{2+}, Hg^{2+}, Sr^{2+}, La^{3+} and Lu^{3+}, by ^{1}H,^{15}N HMQC NMR experiments. The effects of these ions on the substrate-binding ability of calmodulin have also been studied by fluorescence spectroscopy of the single tryptophan residue in a 22-residue synthetic peptide encompassing the skeletal muscle myosin light chain kinase calmodulin-binding domain. Most of these metal ions can activate a calmodulin target enzyme to some extent, though they bind to calmodulin in a different manner. Mg^{2+}, which is of direct physiological interest, has a distinct site-preference for calmodulin, as it shows the highest affinity for site I in the N-terminal domain, while the C-terminal sites III and IV are the high affinity binding sites for Ca^{2+} (as well as for Cd^{2+}). At a high concentration of Mg^{2+} and a low concentration of Ca^{2+}, calmodulin can bind Mg^{2+} in its N-terminal lobe while the C-terminal domain is occupied by Ca^{2+}; this species could exist in resting cells in which the Mg^{2+} level significantly exceeds that of Ca^{2+}. Moreover, our data suggest that the toxicity of Pb^{2+}—which, like Sr^{2+}, binds with an equal and high affinity to all four sites—may be related to its capacity to tightly bind and improperly activate calmodulin.

Keywords: calmodulin, fluorescence spectroscopy, metal ions, NMR

Abbreviations: CaM, calmodulin; EDTA, ethylenediaminetetraacetic acid; Gly, glycine; HMQC, heteronuclear multiple quantum coherence; MLCK, myosin light chain kinase; NMR, nuclear magentic resonance; Trp, tryptophan.

Introduction

The calcium ion is an important intracellular messenger involved in signal transduction processes. Normally, the free Ca^{2+} level in most resting cells is around 10^{-7} M. The intracellular Ca^{2+} concentration can increase rapidly to 10^{-6}–10^{-5} M when the cell is excited by hormones, nerve impulses, or other stimuli. The increase of the cytoplasmic Ca^{2+} level gives rise to changes in a wide range of biological events, including muscle contraction, production of nitric oxides, oxidative phosphorylation, protein phosphorylation, DNA replication and cell proliferation. Many of the Ca^{2+} effects are mediated by a class of intracellular helix–loop–helix Ca^{2+}-binding proteins of which calmodulin (CaM) appears to be the most versatile and ubiquitous (Vogel 1994, Vogel & Zhang 1995, Ikura 1996).

CaM is a highly conserved secondary messenger protein which has been found in almost every eukaryotic cell. More than thirty proteins and enzymes with various cellular functions have been found to be activated by CaM. The vast majority of

Address for correspondence: H.J. Vogel, Department of Biological Sciences, The University of Calgary, Calgary, Alberta, T2N 1N4, Canada. Tel: (+1) 403 220 6006; Fax: (+1) 403 289 9311; e-mail: vogel@acs.ucalgary.ca

these target enzymes are activated only by Ca^{2+}-saturated CaM, although apo-CaM has also been found to interact with a few proteins. Ca^{2+}–CaM induces amphiphilic α-helices in the target enzymes via hydrophobic and ion-pair interactions (O'Neil & DeGrado 1990, Crivici & Ikura 1995, Vogel & Zhang 1995). X-ray and NMR studies have shown that Ca^{2+}–CaM contains two lobes which are linked by a long α-helix in the crystal structure and by a flexible linker in solution (Babu *et al*. 1988, Barbato *et al*. 1992). Each lobe has two Ca^{2+}-binding sites which show typical helix–loop–helix structures often referred to as "EF-hands" (Kawasaki & Kretsinger 1994); these motifs are highly conserved throughout this group of proteins. There is a large hydrophobic patch on the surface of each domain of CaM which is essential for substrate binding. The structure of apo-CaM has also been determined recently (Kuboniwa *et al*. 1995, Zhang *et al*. 1995); its overall shape is similar to that of Ca^{2+}–CaM, but apo-CaM does not have the large hydrophobic surfaces, as a result of different interhelical angles within the lobes. The binding of Ca^{2+} ions triggers the reorientation of the helices, resulting in the exposure of the hydrophobic surfaces on both domains, which enables the protein to recognize its substrates (Vogel 1994, Zhang *et al*. 1995, Ikura 1996). Thus, the Ca^{2+}-binding process and the subsequent conformational changes are key features for the target enzyme activation mediated by CaM.

Ca^{2+} ions bind to apo-CaM in a step-wise manner: first, two Ca^{2+} ions bind to the C-terminal domain (sites III and IV) cooperatively; this is followed by the binding of the next two Ca^{2+} ions to the N-terminal domain (sites I and II), also in a cooperative fashion (Andersson *et al.* 1983, Ikura *et al.* 1983). Cooperativity of metal ion binding between the two lobes has been found in the presence of substrate proteins (Hiraoki & Vogel 1987, Vogel 1994). This positive cooperativity within four Ca^{2+}-binding sites allows CaM to function effectively as an on/off switch over the narrow range of Ca^{2+} concentrations that distinguishes resting and stimulated cells (10^{-7} and 10^{-6} M, respectively). Although Ca^{2+}–CaM plays many important roles in signal transduction pathways, Ca^{2+} does not seem to be the exclusive ion that can activate CaM. In contrast, CaM displays a surprisingly broad specificity for various metal ions. More than ten different metal ions have been found to be able to substitute for Ca^{2+} in CaM. Most of these metal ions can enable CaM to activate one of its target enzymes, the CaM-dependent cyclic nucleotide phospho-diesterase, to some extent (Chao *et al*. 1984). These authors also reported relative binding constants which were determined by competition dialysis equilibrium measurements (Chao *et al*. 1984). The capacity to substitute for Ca^{2+} is probably based on the similarity in ionic radii with Ca^{2+} (0.99 Å). The presence of many other metal ions in the physiological environment suggests that CaM might be binding metal ions other than Ca^{2+} ions, expecially in resting cells in which the Ca^{2+} concentration is particularly low. Thus, it is of importance to investigate the general metal ion binding properties of CaM. In this work, we have studied the binding of various metal ions, such as K^+, Na^+, Mg^{2+}, Zn^{2+}, Cd^{2+}, Pb^{2+}, Hg^{2+}, Sr^{2+}, La^{3+} and Lu^{3+}, to CaM with NMR techniques (the ionic radii of these different metal ions are listed in Table 1). The effects of these ions on the substrate-binding ability of CaM have also been studied by fluorescence spectroscopy studies of the binding of the CaM-binding domain peptide derived from skeletal muscle MLCK. This peptide contains a single Trp residue, while CaM is devoid of Trp, thus making it straightforward to study its binding by fluorescence spectroscopy. Our data show that many of these metal cations can bind to CaM, but that they all bind in a different manner and that they allow binding of CaM to the MLCK peptide to some extent.

Materials and methods

Materials

$CaCl_2$, $MgCl_2$, $ZnCl_2$, $CdCl_2$, $Pb(NO_3)_2$, $HgCl_2$, NaCl KCl, $SrCl_2$, $LuCl_3$ and $LaCl_3$ were obtained from Aldrich (Milwaukee, WI, USA), at the highest available quality. ^{15}N-glycine and D_2O (99.9%) were purchased from Cambridge Isotope Laboratories (Andover, MA, USA). The MLCK peptide, a 22-residue peptide with sequence

Table 1. Ionic radii of various metal ions used in this work*

Cation	Ionic radius (Å)
Na^+	0.97
K^+	1.33
Mg^{2+}	0.66
Zn^{2+}	0.72
Cd^{2+}	0.97
Ca^{2+}	0.99
Hg^{2+}	1.10
Sr^{2+}	1.13
Pb^{2+}	1.20
La^{3+}	1.02
Lu^{3+}	0.85

*Taken from CRC Handbook.

KRRWKKNFIAVSAANRFKKISS, was obtained from the Peptide Synthesis Facility at Queens University (Kingston, ON, Canada); it contains residues 577 to 598 of skeletal muscle MLCK, which constitutes its CaM-binding domain (Blumenthal *et al.* 1988). The *E. coli* strains, MM294 and D139G (a Gly auxotroph) were used as hosts to express nonlabelled and ^{15}N-Gly labelled CaM, respectively. CaM was expressed in *E. coli* and purified by hydrophobic affinity chromatography as previously described (Zhang *et al.* 1994). All the glassware and plastic tubes used were acid-washed to reduce metal ion contamination.

NMR spectroscopy experiments

Apo-CaM was prepared by passing a solution of CaM through a Chelex-100 column (Bio-Rad, Hercules, CA, USA) equilibrated with 50 mM NH_4HCO_3 buffer, pH 8.0. Typically, NMR samples were prepared by dissolving 15 mg lyophilized apo-CaM in 500 μl 90% H_2O–10% D_2O, followed by the adjustment of the pH to 6.4. All samples, except those used for the titrations with K^+ and Na^+, also contained 0.1 M KCl to mimic physiological conditions. The concentration of CaM was determined by optical absorbance using a $\Delta E^{1\%}_{276/320}$ value of 1.8. The binding of the metal ions to CaM was studied by titrating the apo-CaM sample with the metal ions of interest. The titrations were monitored by ^{1}H, ^{15}N HMQC NMR experiments. Microlitre amounts of the stock solution of the metal ions (0.1–3 M) were added to the desired concentration at each titration point, while the pH was maintained at 6.4. If some protein precipitated during the titration, the sample was centrifuged at 14 000 rpm in a microcentrifuge and the supernatant was used for the next NMR experiment. All NMR spectra were recorded at 25°C on a Bruker AMX-500 spectrometer. The ^{1}H, ^{15}N HMQC data were recorded using the pulse sequence described by Sklenár & Bax (1987). The spectra were processed on a Silicon Graphics Indy R5000 computer using NMRpipe software. The assignments of the Gly residues of the apo- and calcium-forms of CaM were taken from Ohki *et al.* (1997) and Ikura *et al.* (1991), respectively.

Fluorescence spectroscopy experiments

Fluorescence spectroscopy experiments were performed on a Hitachi F-2000 Fluorescence spectrophotometer. The concentration of the peptide was determined by optical absorbance using ϵ_{280}=5500 cm^{-1} M^{-1}. The sample buffer containing 10 mM Tris–Cl (pH 7.4), 0.1 M KCl was passed through a Chelex-100 column (Bio-Rad) to remove divalent and trivalent cations. Apo-CaM (10 μM) and MLCK peptide (10 μM) were incubated in the sample buffer with or without 2 mM $CaCl_2$ (or $MgCl_2$, $ZnCl_2$, $CdCl_2$, $Pb(NO_3)_2$, $HgCl_2$, $SrCl_2$, $LuCl_3$, $LaCl_3$) at room temperature for at least 60 min before the spectra were recorded. The samples were spun at 14 000 rpm on a bench top centrifuge if protein precipitation was observed. The samples were excited at 295 nm and the emission spectra were recorded in the range 310–450 nm. The excitation and emission slit widths were 1 nm, and the emission spectra scanning was done at 60 nm min^{-1} with an 1 cm path length cuvette.

Results

There is a total of eleven Gly residues in CaM. Table 2 shows that all four Ca^{2+}-binding loops of CaM have two Gly residues at homologous positions; these are highly conserved in all EF-hand Ca^{2+}-binding motifs (Kawasaki & Kretsinger 1994). Two additional Gly residues (G40 and G113) are located in homologous positions in the loops that connect the two helix–loop–helix structures in each lobe of CaM. The final G33 residue is located close to the first calcium binding loop. Thus, the Gly residues were chosen as convenient reporter groups to monitor the binding of metal ions to the four Ca^{2+}-binding loops of CaM. Figure 1 shows NMR spectra of the titration of ^{15}N-Gly labelled apo-CaM with Ca^{2+} ions. Obvious changes were observed when the first two equivalents of Ca^{2+} were added to CaM, and these changes were limited to the C-terminal domain of the protein. As can be seen in Figure 1B, the intensity of peaks G132 and G134 (site IV) decreased (as measured from the number of peak contours) as the Ca^{2+} concentration increased, and new peaks emerged at the known positions of G132 and G134 in the Ca^{2+}-saturated CaM spectrum. G98 (site III), which is not observed in the apo-CaM spectrum, also appeared at its known position for Ca^{2+}–CaM. G96 (site III) disappeared gradually and a new peak emerged at the correct position corresponding to G96 in Ca^{2+}–CaM, which demonstrated a typical slow-exchange that was also observed for peak G113, the Gly residue in the linker region between site III and site IV. When more Ca^{2+} was added, the resonances of the Gly residues in the N-terminal domain were also altered until the Ca^{2+} concentration reached four equivalents (Figure 1C). Intermediate-exchange was observed for most Gly residues in the N-terminal domain during this part of the Ca^{2+} titration.

A titration of apo-CaM with Mg^{2+} was also performed. With the addition of the first equivalent

Table 2. Primary structure of the four Ca^{2+}-binding loops of CaM

Site I	20	D	K	D	**G**	D	**G**	T	I	T	T	K	E	31
Site II	56	D	A	D	**G**	N	**G**	T	I	D	F	P	E	67
Site III	93	D	K	D	**G**	N	**G**	Y	I	S	A	A	E	104
Site IV	129	N	I	D	**G**	D	**G**	Q	V	N	Y	E	E	140

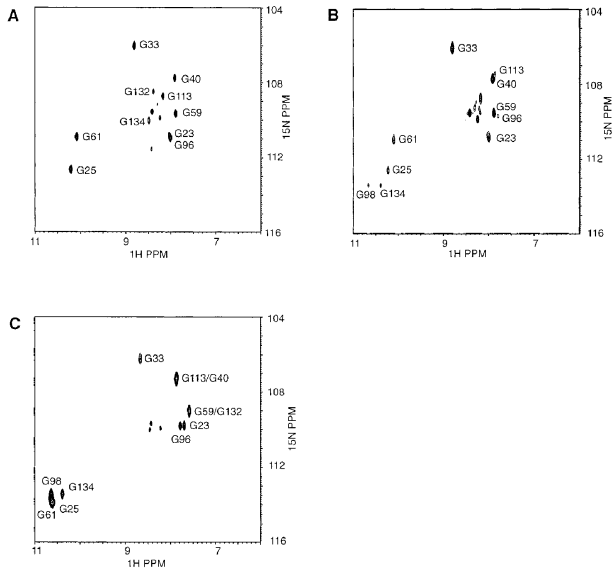

Figure 1. 2D ^{1}H, ^{15}N HMQC spectra of the titration of CaM (1.47 mM, pH 6.4) with: (A) zero equivalents; (B) two equivalents; and (C) four equivalents of $CaCl_2$.

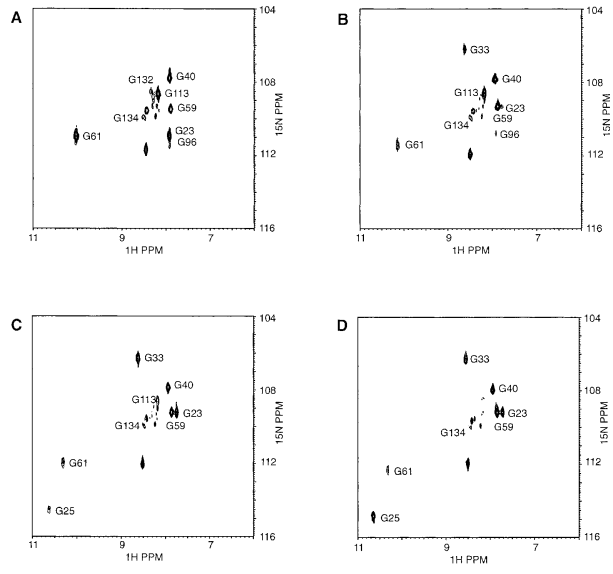

Figure 2. 2D ^{1}H, ^{15}N HMQC spectra of the titration of CaM (1.09 mM, pH 6.4) with: (A) one equivalent; (B) five equivalents; (C) 15 equivalents; and (D) 75 equivalents of $MgCl_2$. See Figure 1A for the specturm of apo-CaM.

of Mg^{2+}, peak G25 (site I) disappeared while G33 broadened. The change of G23 (site I) was somewhat ambiguous since it overlapped with G96 in the apo-CaM spectrum (Figure 1A). The peak for G132 (site IV) decreased when a second equivalent of Mg^{2+} was added, however, with no significant changes in G134 (site IV). CaM was further titrated to five equivalents of Mg^{2+}, with a new peak for G23 emerging on the spectrum, while peak G96 was broadening (Figure 2B). G96 completely disappeared at eight equivalents of Mg^{2+}, while G33 reappeared at a new position slightly different from the original one. Another new peak for G25 emerged at 15 equivalents of Mg^{2+} (Figure 2C). No further significant changes were observed in the spectra, except for a decrease of the intensity for G113 when the Mg^{2+} level increased up to 75 equivalents (Figure 2D). These data suggest that Ca^{2+}-binding site I located in the N-terminal domain of CaM has the highest affinity for Mg^{2+}. The Ca^{2+}-binding sites in the C-terminal domain, namely sites III and IV, displayed a lower affinity for Mg^{2+} ions. Thus, Mg^{2+} has a different site-preference compared to Ca^{2+}. We also performed a titration of CaM with Ca^{2+} in the presence of a high Mg^{2+} concentration (75 equivalents) to investigate if the presence of Mg^{2+} ions affects the Ca^{2+}-binding properties of the protein. Upon addition of the first equivalent of Ca^{2+}, five small new peaks emerged; these peaks were at the exact positions of G96, G98, G113, G132 and G134 in the Ca^{2+}–CaM spectrum, suggesting regular incorporation of Ca^{2+} into the C-terminal domain. When the second equivalent of Ca^{2+} was added, the intensity of these new peaks increased (Figure 3A). The resonances from the C-terminal domain were at the Ca^{2+}-saturated positions and did not change with the further addition of Ca^{2+} ions. Most peaks of Gly residues in the N-terminal domain were at the same positions as in apo-CaM, except for G23 and G25, indicating that site I was still occupied by Mg^{2+}. These two peaks kept shifting (fast-exchange) when more Ca^{2+} was added up until four to six equivalents, while G33 broadened beyond detection (Figure 3B). At 10 equivalents of Ca^{2+}, G23 and G25 shifted to their final positions and G33 reappeared (Figure 3C). At this point, the spectrum superimposed perfectly on the spectrum of Ca^{2+}-saturated CaM. The shifting of the G23 and G25 resonances indicated fast-exchange between the apo and Ca^{2+}-bound states of the N-terminal domain on the NMR time scale, which further suggested that binding of Ca^{2+} to the N-terminal domain was relatively weak in the presence of high concentrations of Mg^{2+}.

Intermediate- to fast-exchange was observed during the titration with Zn^{2+} (data not shown). G23 started shifting and broadening at one equivalent of Zn^{2+}, and disappeared at two equivalents. G25 and G33 shifted in the same direction while maintaining

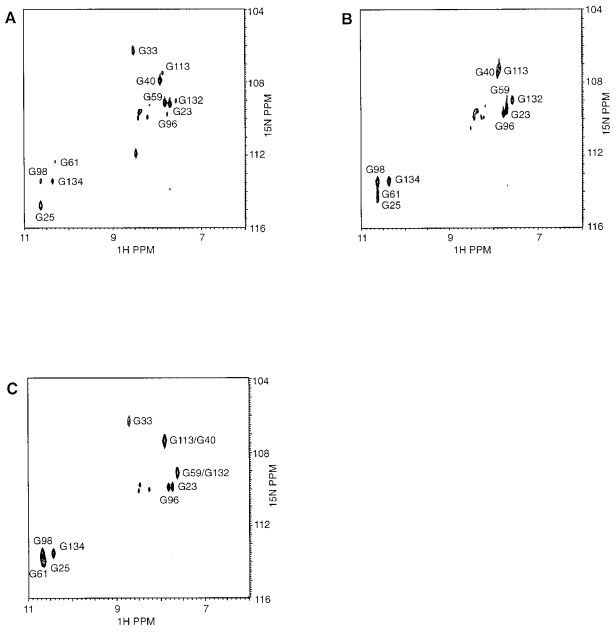

Figure 3. 2D ^{1}H, ^{15}N HMQC spectra of the titration of CaM (1.09 mM, pH 6.4) with $CaCl_2$ in the presence of 90 mM $MgCl_2$. (A) two equivalents of $CaCl_2$. G23 and G25 are in positions different from that of apo-CaM (Figure 1A) or Ca^{2+}–CaM (figure 1C). (B) four equivalents of $CaCl_2$. Note the shifting of G23 and G25, as well as the disappearance of G33. (C) 10 equivalents of $CaCl_2$. See text for details.

their intensities until the Zn^{2+} concentration reached four equivalents. G59 and G61 also shifted slightly as the level of Zn^{2+} increased from one to two equivalents. G132 faded away when one equivalent of Zn^{2+} was added. G113 and G134 remained unchanged during addition of the first equivalent, and broadened when the Zn^{2+} concentration exceeded three equivalents. G96 was shifting during the whole titration with the same intensity. G40 did not change during the titration of Zn^{2+}. These data suggest that Zn^{2+} ions could interact with CaM; the fast-exchange observed during the titration indicated that the interactions were relatively weak.

Apo-CaM was also titrated with increasing concentrations of K^+ and Na^+. No significant changes were observed in the HMQC spectrum of ^{15}N-Gly labelled CaM during a titration with K^+ up to 150 mM. However, small changes could be detected upon the addition of Na^+ (data not shown). The peaks for G23 and G96 overlapped when no Na^+ ions were present; these two peaks began to separate when the Na^+ concentration was increased to four to eight equivalents, and evolved into two distinct peaks at over 20 equivalents of Na^+. A small new peak emerged at 10.22 ppm (^{1}H) and 111.89 ppm (^{15}N) when the Na^+ concentration exceeded 50 equivalents. This new peak probably arose from G98, which was not detectable in the apo-CaM spectrum.

The results obtained during a titration of apo-CaM with Cd^{2+} were similar to those of Ca^{2+}. The resonances of the Gly residues from the C-terminal domain decreased in intensity as soon as Cd^{2+} was added. At two equivalents of Cd^{2+}, five new peaks appeared for G96, G98, G113, G132, and G134. The peaks for the N-terminal Gly residues started to change as the titration proceeded. G23, G25 and G59 kept shifting when the Cd^{2+} concentration increased from two to four equivalents. G61 had disappeared at three equivalents of Cd^{2+}, and reappeared at four equivalents. Several new peaks at the right-bottom corner of the spectrum kept shifting when Cd^{2+} was further added, suggesting the presence of additional binding sites for this metal ion.

NMR titrations with Pb^{2+} could not be performed beyond two equivalents because the Pb^{2+} ions caused aggregration and precipitation of CaM. However, the changes in the spectra of the first two equivalents were obvious: G23 (site I), G59 (site II), G96 (site III) and G132 (site IV) disappeared at one equivalent of Pb^{2+}, followed by the disappearance of G25 (site I), G61 (site II), G98 (III) and G134 (site IV) at two equivalents of Pb^{2+} (Figure 4). These data suggest that all four sites of CaM have the same affinity for Pb^{2+} ions. It also seemed that all four sites were affected when the first equivalent of Sr^{2+} was added during a titration with Sr^{2+}. G23, G25, G61, G96 and G132 all decreased, while G33 and G59 shifted to new positions. Some of the peaks which had disappeared reappeared in the spectrum when a second equivalent of Sr^{2+} was added; the intensities of these new peaks increased as more Sr^{2+} was added. These data showed that Sr^{2+} binds to CaM in the same manner as Pb^{2+}, which has an equally high affinity for all four sites in CaM.

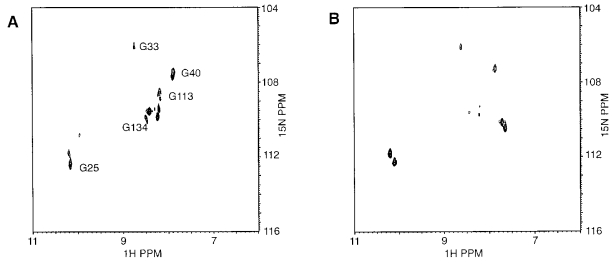

Figure 4. 2D ^{1}H, ^{15}N HMQC spectra of the titration of CaM (1.28 mM, pH 6.4) with: (A) one equivalent; and (B) two equivalents of $Pb(NO_3)_2$. See Figure 1A for the spectrum of apo-CaM.

The titration with Hg^{2+} could be divided into two stages. At low Hg^{2+} concentrations (two to three equivalents), G132 and G134 (site IV) disappeared while G113 slightly shifted. No other significant changes were observed until the Hg^{2+} level was very high (12 equivalents), when G25 (site I) and G61 (site II) were broadening, while G23 (site I) and G59 (site II) remained unchanged. Thus, site IV probably had the highest affinity for Hg^{2+}, while sites I and II showed much lower affinities. Competition experiments showed that Ca^{2+} could readily displace Hg^{2+} and Cd^{2+}, but not Pb^{2+} (data not shown, see also Aramini *et al*. 1996).

In the titration experiments with the largest lanthanide ion La^{3+} and apo-CaM, G132 and G134 (site IV) were the first resonances to lose intensity. The peaks representing the Ca^{2+}-binding sites in the N-terminal domain, G23, G25 (site I), G59 and G61 (site II), also started to lose intensity, followed by the relocating of peak G96 (site III) as the titration proceeded. These results suggested that La^{3+} can bind to all four sites in CaM, but with different affinity. Site IV showed the higher La^{3+} binding ability, followed by site I and site II, while site III had the lowest affinity for La^{3+}. Apo-CaM was also titrated with the other diamagnetic lanthanide ion Lu^{3+}. The disappearance of G132 and G134 (site IV) followed the addition of one equivalent of Lu^{3+}. All the other peaks, except G33, changed position when more Lu^{3+} was added. G23, G25 (site I), G61 (site II) and G113 disappeared, with some new peaks emerging. G40, G59 (site II) and G96 (site III) shifted to new positions. These results suggest that site IV has the highest affinity for the smallest lanthanide ion Lu^{3+}, while the other three sites have an almost equal affinity for this metal ion.

The effects of different divalent and trivalent metal ions on the substrate-binding abilities of CaM were investigated by fluorescence spectroscopy. The synthetic MLCK peptide was chosen as a model substrate because it contains a single Trp residue. Thus, the binding of the MLCK peptide to CaM can be monitored by studying the fluorescence change of this Trp residue upon binding to CaM. The binding of Ca^{2+} to CaM induces a major conformational change in the protein, resulting in the exposure of the large hydrophibic surfaces which are essential for the peptide binding. When the MLCK peptide binds CaM, the Trp residue moves from a polar environment into a nonpolar hydrophobic environment (Ikura *et al*. 1992, Crivici & Ikura 1995), which causes a large blue shift and an increase in the intensity of the emission spectrum (Yuan *et al*. 1998). This large blue shift and intensity change are not observed when the peptide, apo-CaM and a large excess of EDTA are incubated. Some of the emission spectra are shown in Figure 5. Unfortunately, the other metal ions in our studies caused protein precipitation during the incubation under these experimental conditions, which significantly lowered the fluorescence intensity (data not shown). However, the blue shift can still be observed for these metal ions (Table 3). Our data indicate that most of the divalent and trivalent metal ions can induce a blue shift and an increase in intensity in the emission spectrum, except for Mg^{2+}, suggesting that most of these metal ions should also be able to activate CaM to some extent.

Discussion

The metal ions included in this study can arbitrarily be divided into four groups: Group A, Ca^{2+}, Mg^{2+} and Zn^{2+}; Group B, K^{+} and Na^{+}; Group C, Cd^{2+}, Pb^{2+} and Hg^{2+}; and Group D, Sr^{2+}, La^{3+} and Lu^{3+}. The divalent metal ions of Group A naturally occur in cells and have relatively high intracellular concentrations; Group B is comprised of monovalent cations that have a high physiological concentration; the metal ions in Group C are serious environmental pollutants and are toxic to cells; Group D includes divalent and trivalent cations that have often been used as calcium analogs in various studies, such as fluorescence and luminescent spectroscopy (Kilhoffer *et al*. 1980, Wang *et al*. 1982, Mills & Johnson 1985). Our studies on the binding of these metal ions to CaM will shed light on the role that different metal ions can play in Ca^{2+} signal transduction pathways.

In Group A, Ca^{2+} is the natural 'substrate' of CaM. The binding of Ca^{2+} to CaM has been well

Table 3. Wavelength of the MLCK peptide emission peak with CaM in the presence of various metal ions

Metal ions	Wavelength (nm)
None	342
Mg^{2+}	341
Zn^{2+}	334
Cd^{2+}	332
Ca^{2+}	332
Hg^{2+}	340
Sr^{2+}	332
Pb^{2+}	332
La^{3+}	332
Lu^{3+}	334

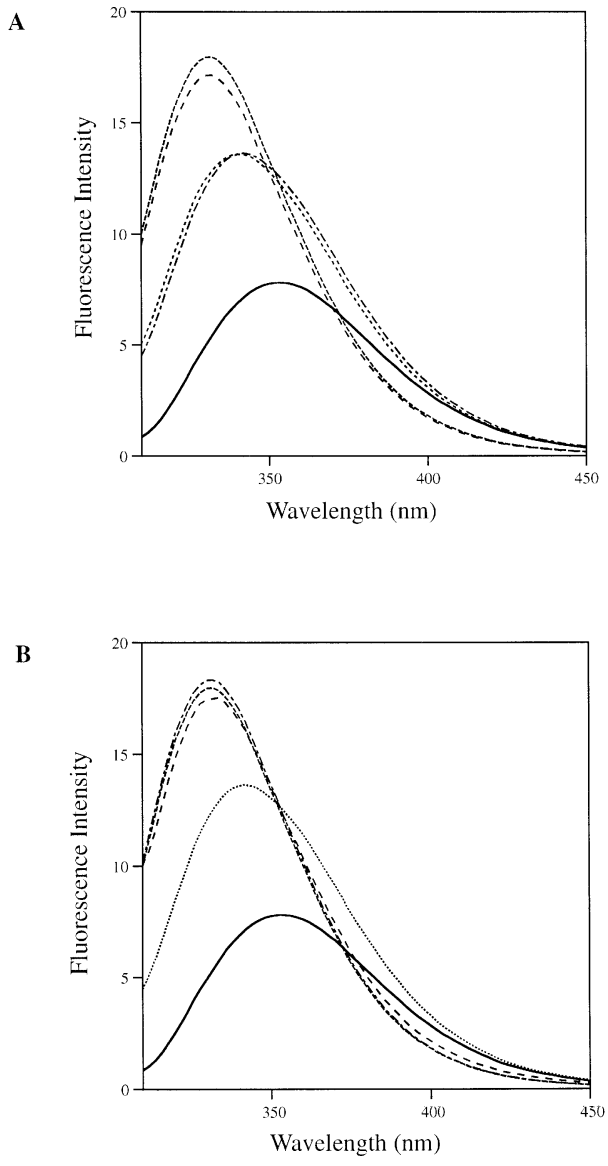

Figure 5. Fluorescence emission spectra showing the effects of various metal ions on the substrate-binding ability of CaM monitored by the fluorescence of the Trp residue in the MLCK peptide. (A) Trp fluorescence of the MLCK peptide (———) showed a larger blue shift and larger intensity increase when the peptide was incubated with Ca^{2+}–CaM (- - - - - -) rather than with apo-CaM (– – – – –). The spectra of the samples incubated in the presence of Mg^{2+} and Sr^{2+} are shown by (--------) and (– – – – –), respectively. (B) Fluorescence emission spectra of the MLCK peptide (———), the peptide preincubated with apo-CaM (.....), and CaM in presence of Ca^{2+} (--------), Zn^{2+} (– – – – –) and Cd^{2+} (– - – - –).

studied. The Ca^{2+} titration in this study (Figure 1) confirmed the known Ca^{2+}-binding properties of apo-CaM: at least a ten-fold higher affinity for the two C-terminal sites and lower affinity for the N-terminal sites. The slow-exchange observed during the titration indicated the relatively strong binding of Ca^{2+} to the C-terminal lobe of CaM. The intracellular Ca^{2+} concentration is strictly controlled in cells and constantly fluctuates around the level required to saturate CaM (Ohki *et al.* 1993, Vogel 1994). In the case of Mg^{2+}, the situation is rather different. In most multicellular organisms both the intracellular and extracellular free Mg^{2+} concentrations are maintained at approximately 10^{-3} M, i.e. 10^3–10^4 fold higher than that of Ca^{2+} (Frausto da Silva & Williams 1991). The high intracellular level of Mg^{2+} suggests that Mg^{2+} may substitute for Ca^{2+} inside cells. Tsai *et al.* (1987) have studied the binding of Mg^{2+} to CaM by magnesium-25 NMR. They found that sites in the N-terminal domain have higher affinities for Mg^{2+}; in their studies they treated sites I and II, and sites III and IV as two sets of equivalent sites. Our data are in general agreement with their conclusions. More precisely, we found that site I, but not site II, in the N-terminal domain has the highest affinity for Mg^{2+}, and that the two C-terminal domain sites have lower affinities (Figure 2). The Mg^{2+}–CaM complex cannot bind to a target protein, as our fluorescence experiments demonstrated. The presence of Mg^{2+} ions does not affect the binding of Ca^{2+} to the C-terminal domain of CaM. However, Mg^{2+} can lower the Ca^{2+}-binding affinity of the N-terminal domain because higher Ca^{2+} concentrations (10 equivalents) were required to saturate CaM at a high Mg^{2+} level (Figure 3). These results are consistent with studies performed by Ohki *et al.* (1997), although these authors suggested that site IV might also be a high affinity site for Mg^{2+}. The existence of some 'auxiliary' Mg^{2+}-binding sites in CaM has been suggested. Lafitte *et al.* (1995) found that CaM can bind two Mg^{2+} ions and suggested they bound to 'auxiliary' sites, which are distinct from the four calcium binding loops. However, our data show that Mg^{2+} influences the spectra of the Gly residues in the calcium binding loops, suggesting that Mg^{2+} does enter the loops although it does not coordinate like Ca^{2+} because it does not give a conformational change. This is probably related to the well known property of Mg^{2+} to retain its bound H_2O ligands, while Ca^{2+} readily releases its water molecules (Frausto da Silva & Williams 1991). Furthermore, Ca^{2+} is able to displace Mg^{2+} ions, again arguing against binding of Mg^{2+} to 'auxiliary' sites. Because the binding of all four Ca^{2+} ions is cooperative in the presence of the substrate enzymes, it is possible that a proportion of CaM is always Ca^{2+}-saturated even when the

Ca^{2+} concentration is low. Considering the high intracellular Mg^{2+} level, Ohki *et al.* (1993) suggested that Mg^{2+} can inhibit the formation of the $4Ca^{2+}$–CaM–enzyme complex at lower Ca^{2+} concentrations. Our data support this suggestion: when CaM was half saturated by Ca^{2+} (only the C-terminal domain bound Ca^{2+} ions), CaM could still bind Mg^{2+} in site I of the N-terminal domain. Because Mg^{2+}-bound CaM is not active, the existence of Mg^{2+} in site I might prevent Ca^{2+} ions from binding to the N-terminal domain to 'accidentally' activate CaM when the Ca^{2+} level is low. Thus, the Ca_2^{2+}–Mg_1^{2+}–CaM complex could well be a real form of CaM that exists in the resting cells.

Zn^{2+} is another divalent cation which can have a significant concentration in the cytoplasm (Frausto da Silva & Williams 1991). Zn^{2+} has been found to be able to activate the CaM-dependent phosphodiesterase to a significant extent (Chao *et al.* 1984). The NMR titration of Zn^{2+} with ^{15}N-Gly labelled CaM displayed fast-exchange in the spectra, indicating that the Ca^{2+}-binding loops were affected by addition of Zn^{2+}. However, these data suggest a relatively low affinity for Zn^{2+}. Milos *et al.* (1989) suggested that CaM has six 'auxiliary' cation-binding sites which are different from the four 'capital' Ca^{2+}-binding sites, and that Zn^{2+} can only bind to the 'auxiliary' sites. If this is the case, these 'auxiliary' sites must be located in the vicinity of the 'capital' sites, i.e. the Ca^{2+}-binding loops. Our fluorescence spectroscopy data showed that Zn^{2+} could also bind to a target peptide, suggesting that the binding of Zn^{2+} may still cause productive conformational changes in CaM. This seems to argue for binding directly to the Ca^{2+}-binding loops.

The ions in Group B, K^+ and Na^+, are by far the highest in concentration among various metal ions inside cells (Frausto da Silva & Williams 1991). It had been reported that K^+ can affect the free energy of binding of Ca^+ ions to CaM (Linse *et al.* 1991), suggesting that K^+ might interact with CaM. Our experiments directly monitored the Ca^+-binding loops during the titration with the large K^+ ion. However, no significant changes were observed in the spectra, suggesting that the effects of K^+ on CaM were nonspecific and not caused by direct binding to the binding loops. Unlike K^+, univalent Na^+—which is of similar size to Ca^{2+}—has been found to interact with both domains of CaM through 'true site-binding' sodium-23 NMR studies (Delville *et al.* 1980). Our data did not totally support this conclusion. The ^{15}N-Gly labelled CaM used in our titrations was very sensitive to any 'true site-binding' since each Ca^+-binding loop has two Gly residues in conserved positions. However, only weak interactions were observed between Na^+ and CaM, and these interactions were limited to site III in the C-terminal domain.

In Group C, Cd^{2+} has been proven to be able to serve as a substitute for Ca^{2+} in *in vitro* studies due to the close similarity in ionic radius. Cd^{2+} has frequently been used for cadmium-113 NMR studies because it is a spin 1/2 nucleus which gives simpler NMR spectra than ^{43}Ca, a quadrupolar nucleus (Andersson *et al.* 1983, Thulin *et al.* 1984, Vogel & Forsén 1987). Our titration data proved that the binding of Cd^{2+} to CaM is indeed very similar to that of Ca^{2+}. There were some changes in the spectra when the Cd^{2+} concentrations exceeded four equivalents. These could be due to the existence of the 'auxiliary' sites to which Cd^{2+} could bind as suggested by Milos *et al.* (1989). The binding of Hg^{2+} to CaM was less significant. Site IV had the highest affinity, while sites I and II had much lower affinities. This was rather different from the other heavy metal ion Pb^{2+}. Pb^{2+} is a toxic ion for cells and has been found to be able to substitute for Ca^{2+} in several proteins (Fullmer *et al.* 1985, Goldstein 1993, Simon 1993). Our data showed that all four Ca^{2+}-binding sites could bind Pb^{2+} simultaneously, which was in agreement with previous lead-207 NMR studies (Aramini *et al.* 1996). Although our fluorescence experiments did not clearly show to what extent Pb^{2+} can activate CaM due to the protein precipitation, Chao *et al.* (1984) demonstrated that Pb^{2+} can activate CaM for over 90%. Thus, the toxicity of Pb^{2+} could be caused by its ability for binding and activating CaM. Sr^{2+} appears to bind to CaM in a similar manner as Pb^{2+}, thus these two divalent ions that are significantly larger than Ca^{2+} bind to CaM in similar manner.

Despite the similarity in size, the trivalent lanthanide ions obviously bind to CaM in a different order from calcium; they appear to have a preference for site IV. Thus, caution should be exercised in using this class of metal ions: their favourable spectroscopic properties do not justify their use in this class of proteins, as erroneous results can be obtained (Szebenyi & Moffat 1986, Kumar *et al.* 1991). Similarly, the use of Sr^{2+} as an experimental probe with CaM can lead to erroneous results.

As mentioned in the Introduction, cooperativity in the binding of calcium ions is an important feature of CaM. From our studies it appears that from all the metal ions tested, only Cd^{2+} is capable of reproducing these effects. This justifies the extensive use of cadmium-113 for the studies of metal ion binding

properties of this class of proteins (Vogel & Forsén 1987, Swain *et al*. 1989).

Fluorescence spectroscopy demonstrated that most of these metal ions could support binding of the MLCK peptide to CaM to some extent, although our NMR studies showed that they bound to CaM in different manners. The binding of Ca^{2+} to CaM changes the protein from a 'closed' conformation to an 'open' conformation which exposes a large hydrophobic surface on each domain. This conformational change is critical for proper substrate recognition and subsequent activation. Many metal ions included in this study could interact with CaM in the Ca^{2+}-binding loops, and trigger at least in part the conformational changes resulting in the 'open' or a 'partially-open' conformation which allows the peptide binding to occur.

Acknowledgements

This work was supported by a grant from the Medical Research Council of Canada. HO is the recipient of a studentship from the Alberta Heritage Foundation for Medical Research (AHFMR). HJV is an AHFMR scientist. We thank Dr D. McIntyre for his expertise in NMR instrument operation and maintenance.

References

Andersson A, Forsén S, Thulin E, Vogel NJ. 1983 Cadmium-113 nuclear magnetic resonance studies of proteolytic fragments of calmodulin: assignment of strong and weak cation binding sites. *Biochemistry* **22**, 2309–2313.

Aramini JM, Hiroaki T, Yazawa M, *et al*. 1996 Lead-207 NMR: a novel probe for the study of calcium-binding proteins. *J Biol Inorg Chem* **1**, 39–48.

Babu YS, Bugg CE, Cook WJ. 1988 Structure of calmodulin refined at 2.2 Å resolution. *J Mol Biol* **204**, 191–204.

Barbato G, Ikura M, Kay LE, Pastor RW, Bax A. 1992 Backbone dynamics of calmodulin studied by ^{15}N relaxation using inverse detected two-dimensional NMR spectroscopy: the central helix is flexible. *Biochemistry* **31**, 5269–5278.

Blumenthal DK, Takio K, Edelman AM, *et al*. 1988 Identification of the calmodulin-binding domain of skeletal myosin light chain kinase. *Proc Natl Acad Sci USA* **82**, 3187–3197.

Chao SH, Suzuki Y, Zysk JR, Cheung WY. 1984. Activation of calmodulin by various metal cations as function of ionic radius. *Mol Pharmacol* **26**, 75–82.

Crivici A, Ikura M. 1995 Molecular and structural basis of target recognition by calmodulin. *Annu Rev Biophys Biomol Struct* **24**, 85–116.

Delville A, Grandjean J, Laszlo P, *et al*. 19880 Sodium-23 nuclear magnetic resonance as an indicator of sodium binding to calmodulin and tryptic fragments, in relation to calcium content. *Eur J Biochem* **109**, 515–522.

Fullmer CS, Edelstein S, Wasserman RH. 1985 Lead-binding properties of intestinal calcium-binding protein. *J Biol Chem* **260**, 6816–6819.

Frausto da Silva JJR, Williams RJP. 1991 *The Bioinorganic Chemistry of the Elements*. Oxford: Clarendon Press.

Goldstein GW. 1993 Evidence that lead acts as a calcium substitute in second messenger metabolism. *Neuro Toxicol* **14**, 97–102.

Hiraoki, T, Vogel HJ. 1987 Structure and function of calcium-binding proteins. *J. Cardiovasc Pharm* **10**, S14–S31.

Ikura M. 1996 Calcium binding and conformational response in EF-hand proteins. *Trends Biochem Sci* **21**, 14–17.

Ikura M, Hiraoki T, Hikichi K, *et al*. 1983 Nuclear magnetic resonance studies on calmodulin: calcium-induced conformational change. *Biochemistry* **22**, 2573–2579.

Ikura M, Spera S, Barbato G, *et al*. 1991 Secondary structure and side-chain proton carbon-13 resonance assignments of calmodulin in solution by heteronuclear multidimensional NMR spectroscopy. *Biochemistry* **30**, 9216–9228.

Ikura M, Clore GM, Gronenborn AM, *et al*. 1992 Solution structure of a calmodulin-target peptide complex by multidimensional NMR. *Science* **256**, 632–638.

Kawasaki H, Kretsinger RH. 1994 Calcium-binding proteins. 1. *Protein Profile* **1**, 343–390.

Kilhoffer MC, Demaille JG, Gerard D. 1980 Terbium as a luminescent probe of calmodulin calcium-binding sites. *FEBS Lett* **116**, 269–272.

Kuboniwa H, Tjandra N, Grzesiek S, *et al*. 1995 Solution structure of calcium-free calmodulin. *Nature Struct Biol* **2**, 768–776.

Kumar VD, Lee L, Edwards BF. 1991 Refined crystal structure of ytterbium-substituted carp parvalbumin 4.25 at 1.5 Å, and its comparison with the native and cadmium-substituted structures. *FEBS Lett* **283**, 311–316.

Lafitte D, Capony JP, Grassy G, Haiech J, Calas B. 1995 Analysis of the ion binding sites of calmodulin by electrospray ionization mass spectrometry. *Biochemistry* **34**, 13825–13832.

Linse S, Helmersson A, Forsén S. 1991 Calcium binding to calmodulin and its globular domains. *J Biol Chem* **266**, 8050–88054.

Mills JS, Johnson JD. 1985 Metal ions as allosteric regulators of calmodulin. *J Biol Chem* **260**, 15100–15105.

Milos M, Comte M, Schaer JJ, Cox JA. 1989 Evidence for four capital and six auxiliary cation-binding sites on calmodulin: divalent cation interactions monitored by direct binding and microcalorimetry. *J Inorg Biochem* **36**, 11–25.

Ohki S, Iwamoto U, Aimoto S, Yazawa M, Hikichi K. 1993 Mg^{2+} inhibits formation of $4Ca^{2+}$-calmodulin-enzyme complex at lower Ca^{2+} concentration. *J Biol Chem* **268**, 12388–12392.

Ohki S, Ikura M, Zhang M. 1997 Identification of Mg^{2+}-binding sites and the role of Mg^{2+} on target recognition by calmodulin. *Biochemistry* **36**, 4309–4316.

O'Neil KT, DeGrado WF. 1990 How calmodulin binds to its target: sequence independent recognition of amphiphilic α-helices. *Trends Biochem Sci* **15**, 59–64.

Simons TJ. 1993 Lead–calcium interactions in cellular lead toxicity. *Neuro Toxicol* **14**, 77–86.

Sklenár V, Bax A. 1987 Spin-echo water suppression for the generation of pure-phase two-dimensional NMR spectra. *J Magn Reson* **74**, 469–479.

Swain AL, Kretsinger RH, Amma EL. 1989 Restrained least squares refinement of native (calcium) and cadmium-substituted carp parvalbumin using X-ray crystallographic data at 1.6-Å resolution. *J Biol Chem* **264**, 16620–16628.

Szebenyi DM, Moffat K. 1986 The refined structure of vitamin D-dependent calcium-binding protein from bovine intestine. Molecular details, ion binding, and implications for the structure of other calcium-binding proteins. *J Biol Chem* **261**, 8761–8777.

Thulin E, Anderson A, Drakenberg T, Forsén S, Vogel HJ. 1984 Metal ion and drug binding to proteolytic fragments of calmodulin: proteolytic, cadmium-113, and proton nuclear magnetic resonance studies. *Biochemistry* **23**, 1862–1870.

Tsai MD, Drakenberg T, Thulin E, Forsén S. 1987 Is the binding of magnesium(II) to calmodulin significant? An investigation by magnesium-25 nuclear magnetic resonance. *Biochemistry* **26**, 3635–3643.

Vogel HJ. 1994 Calmodulin: a versatile calcium mediator protein. *Biochem Cell Biol* **72**, 357–376.

Vogel HJ, Forsén S. 1987 NMR studies of calcium-binding proteins. In: Berliner LJ, Reuben J, eds. *Biological Magnetic Resonance*, vol 7. New York: Plenum Press; 245–307.

Vogel HJ, Zhang M. 1995 Protein engineering and NMR studies of calmodulin. *Mol Cell Biochem* **149/150**, 3–15.

Wang CA, Aquaron RR, Leavis PC, Gergely J. 1982 Metal-binding properties of calmodulin. *Eur J Biochem* **124**, 7–12.

Yuan T, Weljie A, Vogel HJ. 1998 Tryptophan fluorescence quenching by methionine and selenomethionine residues of calmodulin: orientation of peptide and protein binding. *Biochemistry*, **37**, 3187–3195.

Zhang M, Li M, Wang JH, Vogel HJ. 1994 The effect of Met→Leu mutations on calmodulin's ability to activate cyclic nucleotide phosphodiesterase. *J Biol Chem* **269**, 15546–15552.

Zhang M, Tanaka T, Ikura M. 1995 Calcium-induced conformational transition revealed by the solution structure of apo calmodulin. *Nature Struct Biol* **2**, 758–767.